

Suitability of quantum cascade laser spectroscopy for CH₄ and N₂O eddy covariance flux measurements

**P.S. Kroon
A. Hensen
H.J.J. Jonker
M.S. Zahniser
W.H. van 't Veen
A.T. Vermeulen**

Published in Biogeosciences, 4, (2007), 715-728

Suitability of quantum cascade laser spectroscopy for CH₄ and N₂O eddy covariance flux measurements

P. S. Kroon¹, A. Hensen¹, H. J. J. Jonker², M. S. Zahniser³, W. H. van 't Veen¹, and A. T. Vermeulen¹

¹Energy Research Centre of the Netherlands (ECN), Department of Air Quality and Climate Change, The Netherlands

²TU Delft, Department of Multi-Scale Physics, Research Group Clouds, Climate and Air Quality, The Netherlands

³Aerodyne Research, Inc., USA

Received: 20 March 2007 – Published in Biogeosciences Discuss.: 12 April 2007

Revised: 22 August 2007 – Accepted: 29 August 2007 – Published: 31 August 2007

Abstract. A quantum cascade laser spectrometer was evaluated for eddy covariance flux measurements of CH₄ and N₂O using three months of continuous measurements at a field site. The required criteria for eddy covariance flux measurements including continuity, sampling frequency, precision and stationarity were examined. The system operated continuously at a dairy farm on peat grassland in the Netherlands from 17 August to 6 November 2006. An automatic liquid nitrogen filling system for the infrared detector was employed to provide unattended operation of the system. The electronic sampling frequency was 10 Hz, however, the flow response time was 0.08 s, which corresponds to a bandwidth of 2 Hz. A precision of 2.9 and 0.5 ppb Hz^{-1/2} was obtained for CH₄ and N₂O, respectively. Accuracy was assured by frequent calibrations using low and high standard additions. Drifts in the system were compensated by using a 120 s running mean filter. The average CH₄ and N₂O exchange was 512 ngC m⁻² s⁻¹ (2.46 mg m⁻² hr⁻¹) and 52 ngN m⁻² s⁻¹ (0.29 mg m⁻² hr⁻¹). Given that 40% of the total N₂O emission was due to a fertilizing event.

methods are often used to determine integrated emission estimates on a hectare scale that also have continuous coverage in time. Instrumentation is now becoming available that meets the requirements for CH₄ and N₂O eddy covariance (EC) measurements. For example, a limited number of EC measurements have been published using lead salt tunable diode laser (TDL) spectrometers and quantum cascade lasers (QCL) spectrometers (e.g. Smith et al., 1994; Wienhold et al., 1994; Laville et al., 1999; Hargreaves et al., 2001; Werle and Kormann, 2001; Eugster et al., 2007; Neftel et al., 2007).

A TDL spectrometer can obtain similar precision as a QCL spectrometer, however, the big advantage of QCL spectrometers are the better laser frequency stability and freedom from cryogenic cooling cycles that can lead to instability in mode purity and laser frequency. The QCL was first demonstrated in 1994 (Faist et al., 1994). Several studies are performed using QCL spectroscopy e.g. by Nelson et al. (2002) and Jiménez et al. (2005). Nelson et al. (2004) pointed out that the system must satisfy four criteria for performing CH₄ and N₂O EC measurements. First, the continuity criteria which means that the system should be able to operate unattended on a continuous basis at a remote field site. Second, the analyzer response time and the electronic sampling frequency should be both on the order of 10 Hz to evaluate the small eddies as well (Monteith and Unsworth, 1990). Third, the precision of the concentration measurements should be a few parts per thousand of the ambient mixing ratio for CH₄ and one part per thousand for N₂O. A required precision of 4 ppb and 0.3 ppb is derived for CH₄ and N₂O given an average ambient concentration of 1800 ppb and 320 ppb. Finally, the stationarity criteria that indicates the requirement of intermediate term stability against span and minimal drift during a period of atmospheric stationarity on the order of 30 min. Nelson et al. (2004) showed that QCL spectrometers can meet these criteria. This conclusion is mainly based on an experiment with which the system was located in the laboratory. Therefore, it is desirable to validate the suitability of a QCL

1 Introduction

The greenhouse gases methane (CH₄) and nitrous oxide (N₂O) play an important role in global warming with global warming potentials 23 and 296 times greater than CO₂ for 100 years time horizon (IPCC, 2001). Agricultural soils are major sources of both gases (IPCC, 2006). Although, there are significant uncertainties in the estimated CH₄ and N₂O fluxes, mainly owing to a combination of complexity of the source (i.e. spatial and temporal variation), limitations in the measurement equipment and the methodology used to quantify emissions. High-frequency micrometeorological

Correspondence to: P. S. Kroon
(p.kroon@ecn.nl)

Table 1. Main characteristics of Oukoop site in Reeuwijk based on e.g. Veenendaal et al. (2007).

Site	Oukoop in Reeuwijk (NL)
Location	52°01'15" N, 4°01'17" E
Elevation of the polder (m below sea level)	1.6–1.7
Elevation of the ditches (m below sea level)	2.31–2.39
Height of vegetation (m)	0.05–0.35
Mean annual rainfall over 2004 and 2005 (mm yr ⁻¹)	870
Mean temperature over 2004 and 2005 (°C)	10.3
Cow manure application in 2006 (m ³ ha ⁻¹)	55
Artificial fertilizer application in 2006 (kg ha ⁻¹)	320

spectrometer for EC measurements at a remote field site.

This paper discusses the performance of QCL spectrometers for EC measurements using three months of continuous measurements at a dairy farm on peat grasslands in the Netherlands. Moreover, an estimate will be given of CH₄ and N₂O exchange. A description of the experimental site and the climatic conditions is given in Sect. 2. Section 3 is devoted to the instrumentation and the methodology. The results are shown in Sect. 4. The conclusions and discussions are presented in Sect. 5.

2 Experimental site and climatic conditions

The measurements were performed at an intensively managed dairy farm. This farm is located at Oukoop near the town of Reeuwijk in the Netherlands (Coord 52°01'15" N, 4°01'17" E). The surrounding area of the measurement location has soil consisting of a clayey peat or peaty clay layer of up to 0.25 m on up to 12 m eutrophic peat deposits. Rye grass (*Lolium perenne*) is the most dominant grass species with rough bluegrass (*Poa trivialis*) often co-dominant. Clover species constitute less than 1% of the vegetation (Veenendaal et al., 2007). About 21% of the area is open water (Nol et al., 2007¹). The site is located in a polder which means that the water level can be managed. The mean elevation of the polder is between 1.6 and 1.8 m below sea level. Ditch water level in the polder is being kept at -2.39 in winter and -2.31 m in summer (Veenendaal et al., 2007). The climate is temperate and wet, with an average temperature of 10.3°C in 2004 and 2005, and with an average annual precipitation of about 870 mm in 2004 and 2005. The dominating wind direction is southwest (Veenendaal et al., 2007). A summary of the main characteristics is given in Table 1.

Manure and fertilizer are applied about five times a year from February to September. Besides, there are also about

five harvest events. Manure and artificial fertilizer application were about 55 m³ ha⁻¹ yr⁻¹ (253 kgN ha⁻¹ yr⁻¹) and 320 kg ha⁻¹ yr⁻¹ (84 kgN ha⁻¹ yr⁻¹) in 2006. The system operated continuously (coverage of 87%) from 17 August to 6 November 2006. The average temperature over the measurement period was 17°C and 55 kgN ha⁻¹ cow manure was applied on 14 September 2006.

3 Instrumentation and methodology

3.1 Instrumentation

The QCL spectrometer was placed in a container of 2×2×2 m at about 20 m east from the mast. The measurement height was 3 m and the mast was positioned in the middle of the field. Terrain around the towers was flat and free of obstruction for at least 600 m in all directions, except for the container. Wind speed, air temperature, CH₄ and N₂O concentrations were measured with a system consisting of a three-dimensional sonic anemometer (model R3, Gill Instruments, Lymington, UK) and a QCL spectrometer (model QCL-TILDAS-76, Aerodyne Research Inc., Billerica MA, USA).

Figure 1 shows a schematic view of the QCL spectrometer. The QCL spectrometer has a multipass cell with an optical path of 76 m and a volume of 0.5 l maintained between 4.7×10³ Pa (35 Torr) and 4.3×10³ Pa (40 Torr). The QCL spectrometer has two laser positions available that can be used simultaneously. During these experiments only one laser was used which operated at the 1270.8 and 1271.1 cm⁻¹ absorption lines for CH₄ and N₂O, respectively. The performance of the system will be influenced by the use of the second laser. The use of two lasers affects the electronic sampling frequency. Besides, the penalty in signal-noise ratio would be proportionally smaller by the square root of the duty cycle difference (the amount of measurements). If two lasers are sharing the same sweep equally, the signal-noise ratio on both will be increased by $\sqrt{2}$. The reason for not

¹Nol, L. et al.: Effect of land cover data on N₂O inventory in fen meadows, *J. Environ. Qual.*, submitted, 2007.

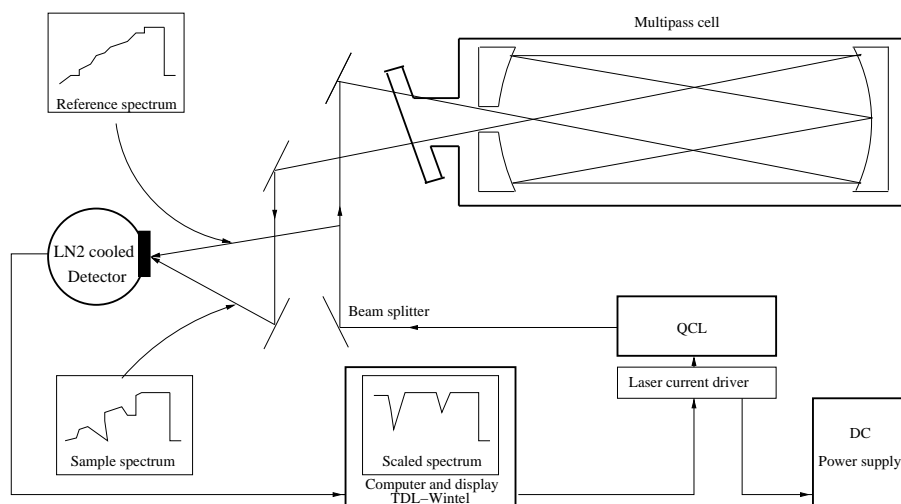


Fig. 1. Schematic view of the QCL spectrometer based on Nelson et al. (2004).

using the second laser in this case was to maximize the signal to noise ratio, which requires the most precision for flux measurements.

The laser was used in pulsed mode. A sequence of laser light pulses, each with duration of about 10 ns, is divided by a beam splitter and sent through the multipass cell and along a bypass. Both beams are detected on a single detector sequentially with the bypass pulse arriving 250 ns before the multipass pulse. The laser frequency is tuned through the absorption lines using a sub-threshold current applied to laser between pulses. The laser light intensity is lower at the start of the pulse sequence and increases towards the end of the pulse sequence. The total width of the scan is close to 0.5 cm^{-1} . This is true for both beams. The bypass signal is used to normalise the signal obtained from the multipass cell. The result is a pattern that shows a relatively constant intensity ratio with a decrease in light intensity passing through the multipass cell at the frequencies of the two absorption lines.

The QCL software, TDL-Wintel, uses spectral parameters listed in the HITRAN database to make a fit to this pattern and derive approximate CH_4 and N_2O gas concentrations (Rothman and Barbe, 2003). With pulsed QCLs, the laser line width is on the same order as the Voigt line width of the absorber, and therefore must be considered in the fitting routine by convolving the laser line shape with the molecular absorbance. The non-Gaussian shape of the laser line profile can result in underestimating the molecular concentration from 10 to 20% depending on the line depth. Calibration with known standards is therefore necessary for greater accuracy.

The detectors of the QCL spectrometer require cooling by liquid nitrogen for maximum sensitivity in the wavelength region. The 0.5 l dewar on the optical table needs to be re-

filled approximately every 24 h. An automated filling unit was used (with a 50 l storage dewar produced by Norhoff, Netherlands). With this setup visits to the instrument were necessary only once a week. In order to minimize drift owing to changing alignment the temperature cover and optical table were maintained at $35 \pm 0.1^\circ\text{C}$ by thin film heaters. The laser electronics were stabilized at $\pm 0.1^\circ\text{C}$ using circulating water bath (Nelson et al., 2004). The water cooling circuit is primarily used to remove the heat generated by the peltier element, which cools the laser. It also stabilizes the temperature of the pulse electronics to provide a more uniform laser output power, and it stabilizes the position of the laser which rest on the peltier element. Without water cooling a variation in reported mixing ratios can occur when ambient temperature surpasses the system temperature as large as $2 \text{ ppb}^\circ\text{C}^{-1}$ for N_2O (Nelson et al., 2004).

The air inlet was located at the sonic height of 3 m above the field. A 25 m PTFE inlet tube with a diameter of 0.25 inch was used. At the QCL spectrometer inlet a $0.01 \mu\text{m}$ filter (DFU filter tube grade BQ, Balston, USA) was used to avoid degradation of the multipass cell mirrors. The flow and cell pressure were controlled with a needle valve at the inlet of the multipass cell. A vacuum pump (TriScoll 600, Varian Inc, USA) with a maximum volume flow rate of 400 l min^{-1} was located downstream of the multipass cell. The QCL spectrometer was calibrated at least once a week using mixtures in N_2/O_2 of 1700 and 5100 ppb for CH_4 and 300 and 610 ppb for N_2O (Scott speciality gasses, Netherlands).

The sonic anemometer data and the QCL spectrometer output were logged using the RS232 output and processed using a data acquisition program developed at ECN, following the procedures of McMillen (1988). Both the QCL spectrometer computer and the EC computer were available for remote control. The electronic sampling frequency of

the QCL spectrometer was not exactly uniform. The average time between two samples was about 0.11 s. The sonic anemometer produced an uniform sampling rate of 20.88 Hz. The data acquisition program saved both the QCL spectrometer and sonic anemometer data in the same file at 20.88 Hz using the last measured concentration value.

3.2 Methods

The net ecosystem exchange (NEE) consists of the sources, the sinks and the surface flux. Horizontal homogeneity, a flat terrain and stationary circumstances were assumed within the average time of 30 min. The storage term was calculated using the average values of CH₄ and N₂O at 3 m height over each 30 min period. The net ecosystem exchange over 30 min of both gasses is given by

$$\underbrace{\int_0^h \overline{S_c} dz}_{\text{NEE}} = \underbrace{\frac{\bar{c}_i - \bar{c}_{i-1}}{T} h}_{\text{Storage}} + \underbrace{\overline{w'c'}|_h}_{\text{Eddy flux}} \quad (1)$$

in which h is the measurement height in m, S_c is the source term in ppb s⁻¹, c is the gas concentration of CH₄ or N₂O in ppb, i indicates the flux number, T is the average time in s and w is the vertical wind velocity in m s⁻¹ (e.g. based on Hoogendoorn and van der Meer, 1991 and Nieuwstadt, 1998).

Evaluation of the eddy flux consisted of different phases. First, the raw data of $w(t)$ and $c(t)$ was analyzed by eye on spikes and malfunctioning. This evaluation was chosen to look in more detail into the data, however, it is very impractical for long term flux measurements. The raw data screening should be done automatically in further research. Then, all concentration data was corrected using a two-point calibration factor based on weekly calibrations. The two-point calibration factor f_{LH} is defined by

$$f_{\text{LH}} = \frac{S_{\text{H}} - S_{\text{L}}}{M_{\text{H}} - M_{\text{L}}} \quad (2)$$

in which S_{L} and S_{H} are the low and high standard values in ppb and M_{L} and M_{H} are the low and high measured values in ppb. The corrected concentration was found using this factor and the following equation

$$C_{\text{cor}} = f_{\text{LH}} C_{\text{uncor}} \quad (3)$$

with C_{uncor} the uncorrected concentration value in ppb and C_{cor} the corrected concentration value in ppb. It was important to correct the data using this factor since the QCL spectrometer does not provide absolute values for the mixing ratios. Next, the time average, which was based on a running mean, and mean removal operations were performed by

$$\tilde{w}_k = \left(1 - \frac{\Delta t}{\tau_f}\right) \tilde{w}_{k-1} + \frac{\Delta t}{\tau_f} w_k \quad (4)$$

$$\tilde{c}_k = \left(1 - \frac{\Delta t}{\tau_f}\right) \tilde{c}_{k-1} + \frac{\Delta t}{\tau_f} c_k \quad (5)$$

$$\overline{w'c'} = \frac{1}{n_s} \sum_{k=1}^{n_s} (w_k - \tilde{w}_k)(c_k - \tilde{c}_k). \quad (6)$$

where k is the sampling number, Δt is the interval between two samples in s, τ_f is the running mean filter time constant in s and n_s is the amount of samples in the average period (Lee et al., 2004). The eddy fluxes F_c were calculated using a 120 s running mean filter time constant and a 30 min average time. Furthermore, the time lag between the sonic anemometer and QCL spectrometer data caused by the length of the sampling tube was determined using the covariance as function of delay time, which is given by

$$F_c = \text{cov}_{wc}(n\Delta t) = \overline{w'_k c'_{k+n\Delta t}} = \frac{1}{n_s} \sum_{k=1}^{n_s} w'_k c'_{k+n\Delta t} \quad (7)$$

where the delay time is defined by $n\Delta t$ in which n denotes the amount of time steps. The absolute maximum in covariance, which represents the eddy flux, occurs at the exact delay time. The exact delay time is dependent on the flow rate in the tube. The flow rate itself is dependent on the resistance of the system, which is mainly dependent on the conditions of the inlet filter. If the inlet filter becomes dirty, the flow rate will decrease.

The storage term was calculated using the QCL spectrometer data according to Eq. (1). The calibrated corrected NEE was given by adding the storage and the eddy flux term. Furthermore, the Webb-correction was partly applied (Webb et al., 1980). The Webb-correction for density fluctuations was not performed since there was a constant temperature and pressure in the sampling cell. However, the Webb-correction for the influence of water vapour fluctuations on trace gas fluxes was applied on the data since the sample was not dried to a constant humidity before the mixing ratio was measured. The Webb-correction was performed using latent heat flux data of the University of Wageningen. These latent heat fluxes were derived using an open path system which was located at the same height and at a distance of about 3 m from the closed path EC system of CH₄ and N₂O. The Webb-correction based on this open path EC system probably overestimated the correction because the 25 m inlet tube of the closed EC system of CH₄ and N₂O attenuated the fluxes. For more information about the open path system the reader is referred to Veenendaal et al. (2007). Moreover, the NEE data were flagged using the instationarity test of Foken and Wichura (1996). Finally, the fetch was checked by a footprint model based on the Kormann-Meixner method (Neftel et al., 2007²; Kormann and Meixner, 2001). The 30 min NEE value was rejected when less than 70% of the flux came from the dairy farm site.

²Neftel, A. et al.: A simple tool for operational footprint evaluations, Environmental Pollution, submitted, 2007.

4 Results

4.1 Performance EC measurements

The required criteria for EC flux measurements including continuity, sampling frequency, precision and stationarity were examined using three months of field measurements. First, the continuity of the system was evaluated. The system operated continuously (total data coverage 87%) at a dairy farm on peat grassland in the Netherlands from 17 August to 6 November 2006 with about one visit per week excluding the intensive campaigns. The system proved to be very stable as far as alignment and laser drift was concerned. The most sensitive part of the system proved to be the liquid nitrogen refilling unit. In summer with high temperatures the container became too hot inside which led to changing alignment. An extra ventilator was installed on the container which proved to be sufficient to keep the temperature inside the container below 35°C.

The validation of the sampling frequency of the system consisted of three parts, namely the electronic sampling frequency, the flow response and the damping. For most conditions a sampling frequency of about 10 Hz is sufficient to perform EC measurements (Ammann, 1998). The electronic sampling frequency is dependent on the complexity of the spectrum and the number of spectral lines included in the fit. Laboratory tests, using the Aerodyne TDL-Wintel software running on a 1 GHz PC showed that 20 Hz acquisition was possible for 2 or 3 gas species simultaneously. Two species were simultaneously measured at an adjusted electronic sampling frequency of 10 Hz during the continuously field measurements. The average time between two samples was about 0.11 s. As a consequence, the contribution to CH₄ and N₂O fluxes of large eddies, with sampling frequencies below 5 Hz, were electronically sampled well, but the contribution of smaller eddies were not.

However, the overall sampling frequency of the system is limited by sampling cell response time rather than the signal processing time. A sampling cell response time ($1/e$) of $\tau=0.08$ s was obtained using the 400 l min⁻¹ Varian vacuum pump with a cell volume of 0.51 in the laboratory. The measured response time implies a volume flow rate of 375 l min⁻¹ which is close to the nominal pumping speed. The response time was not determined in the field since no automatic calibration system was installed. However, the response time in the laboratory and in the field should be probably the same since it should not be a function of the flow rate as long as the pumping speed is constant with the cell pressure. Thus, the effective bandwidth $1/(2\pi\tau)$ is estimated at ~ 2 Hz which is slightly less than the Nyquist frequency of 5 Hz using a sampling rate of 10 Hz.

Nevertheless, the contribution of high frequencies (i.e. the small eddies) to the calculated flux can be decreased by the inlet tube. According to Lenschow and Mann (1994) the damping effect was estimated to be smaller than 50%

for frequencies below 3 Hz when cell pressures were above 4.7×10^3 Pa (35 Torr). In that case, the Reynolds number was higher than 4000. The flow was prevented from becoming less turbulent by regular replacement of the inlet filters. A thorough investigation on the damping effect could be done using an empirical correction approach given by Ammann et al. (2006). This correction approach is based on a comparison of the normalized co-spectrum of wT and $w\text{CH}_4$ or $w\text{N}_2\text{O}$. The wT co-spectrum is calculated from the sonic anemometer with which almost no damping occurred. An estimation of the damping is done using the flux ogives which are given by

$$O_{g_{wc}}^D(f_m) = \sum_{i=1}^m |Co_{wc}(f_i)|$$

$$f_i = \frac{i}{(n_s - 1)\Delta t}; m = 1, 2, \dots, \left[\frac{(n_s - 1)\Delta t}{2\Delta t} \right] \quad (8)$$

where f represents frequency in Hz and Co_{wc} the normalized co-spectrum. The ogive represents the true cumulative contribution of the turbulent eddy frequencies to the flux. The total damping effect is determined by scaling the damped ogive at the low frequencies (up to 0.065 Hz which means a time period of 15 s) to the respective undamped ogive of wT . The damping factor is then indicated by the right-end of the ogive. Figure 2 and 3 show the absolute normalized co-spectra of CH₄, N₂O and wT belonging to 7 October 2006 between 12:00–14:00 which was a neutral period with mean wind velocity of about 7 m s⁻¹ and 8 October 2006 between 00:00–02:00 which was a stable period with mean wind velocity of about 3 m s⁻¹. Besides, the unscaled and scaled ogives are presented in these figures. These analyses were determined using block averaging instead of a running mean filter and an average time of 30 min. The contributions until a sampling frequency of 2 Hz were taken into account. It can be seen that there is almost no difference between the contribution at the high frequencies of the wT flux and the $w\text{CH}_4$ or $w\text{N}_2\text{O}$ flux. Therefore, the damping effects seem to be almost negligible. Although, more analyses should be done to investigate the effect of damping on the flux values for all circumstances.

The system precision and stationarity are strongly dependent on the drift of the instrument. An indication of both properties can be given using an Allan variance analysis (e.g. Allan, 1966; Werle and Slemr, 1991). In this method, the variances in the time series of reported mixing ratio when sampling a constant source from a calibration take are plotted as a function of integration time. The Allan variance decreases with t^{-1} when random noise dominates. This decrease continues to a point at which drift effects start to influence the measurements. Due to instrument drift at longer times the Allan variance increases again. The minimum is indicated by τ_A and σ_A , which represent the stability time in s and the sensitivity in ppb Hz^{-1/2} belonging to this stability time. Apart from this, the y-axis intersection point

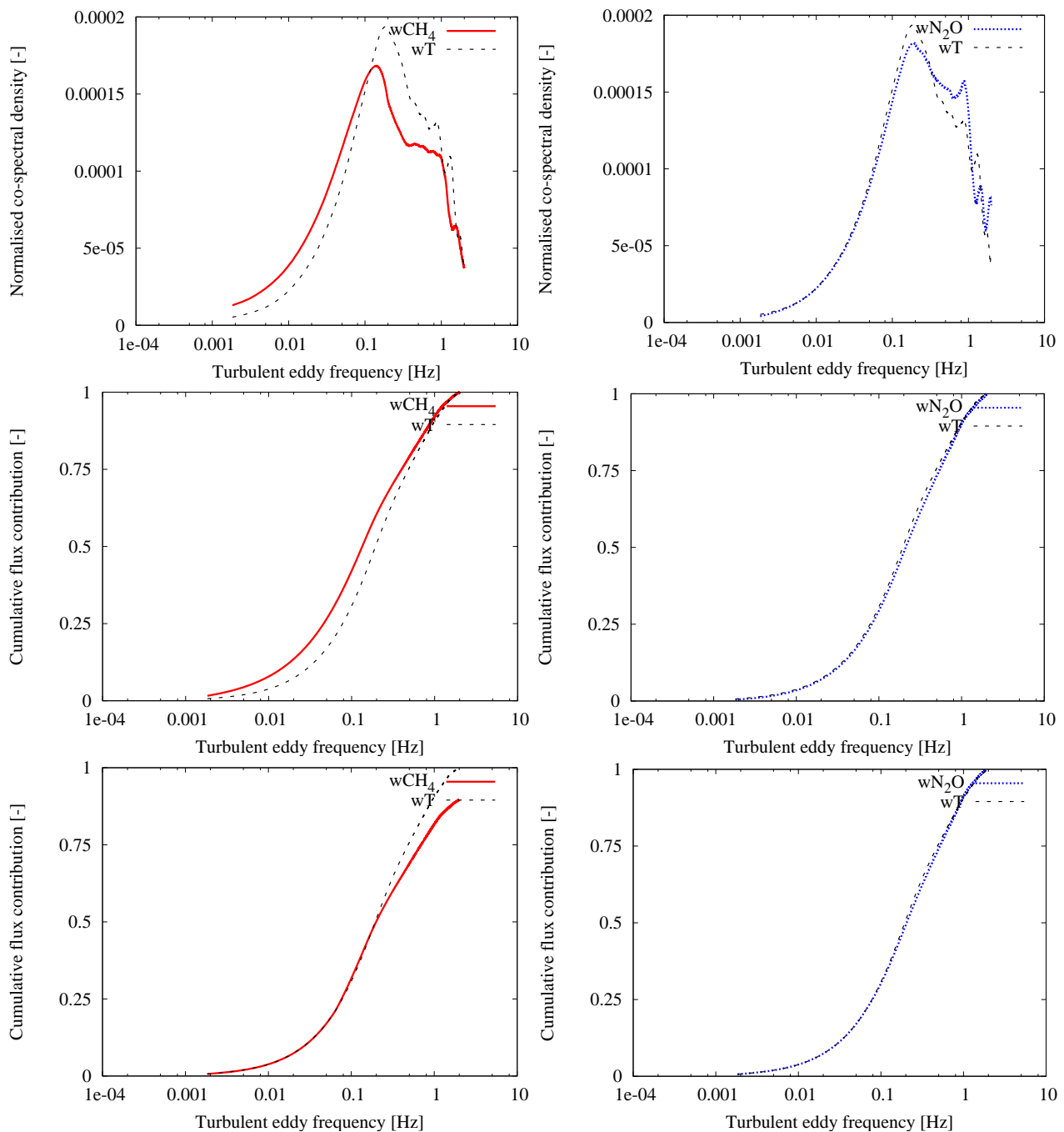


Fig. 2. Comparison of the absolute normalized co-spectra (top), unscaled (middle) and scaled ogives (bottom) with integration started from low frequencies of the heat and CH₄ flux (left) and the heat and N₂O flux (right). The given co-spectra and ogives represent averages over 4 half-hourly measurements on 7 October 2006 between 12:00–14:00.

gives an indication of short term precision of the system in $\text{ppb Hz}^{-1/2}$ using

$$\sigma = \sigma_{1s} f_s^{-1/2} \quad (9)$$

in which f_s is the sampling frequency in Hz. Precision and

stationarity are influenced by drift effects which depend on the instrumental configuration. The most important factor to minimize drift is proper thermal control of optics and the electronics to maintain constant dimensionality and a stable electrical environment of the system. Precision may also be

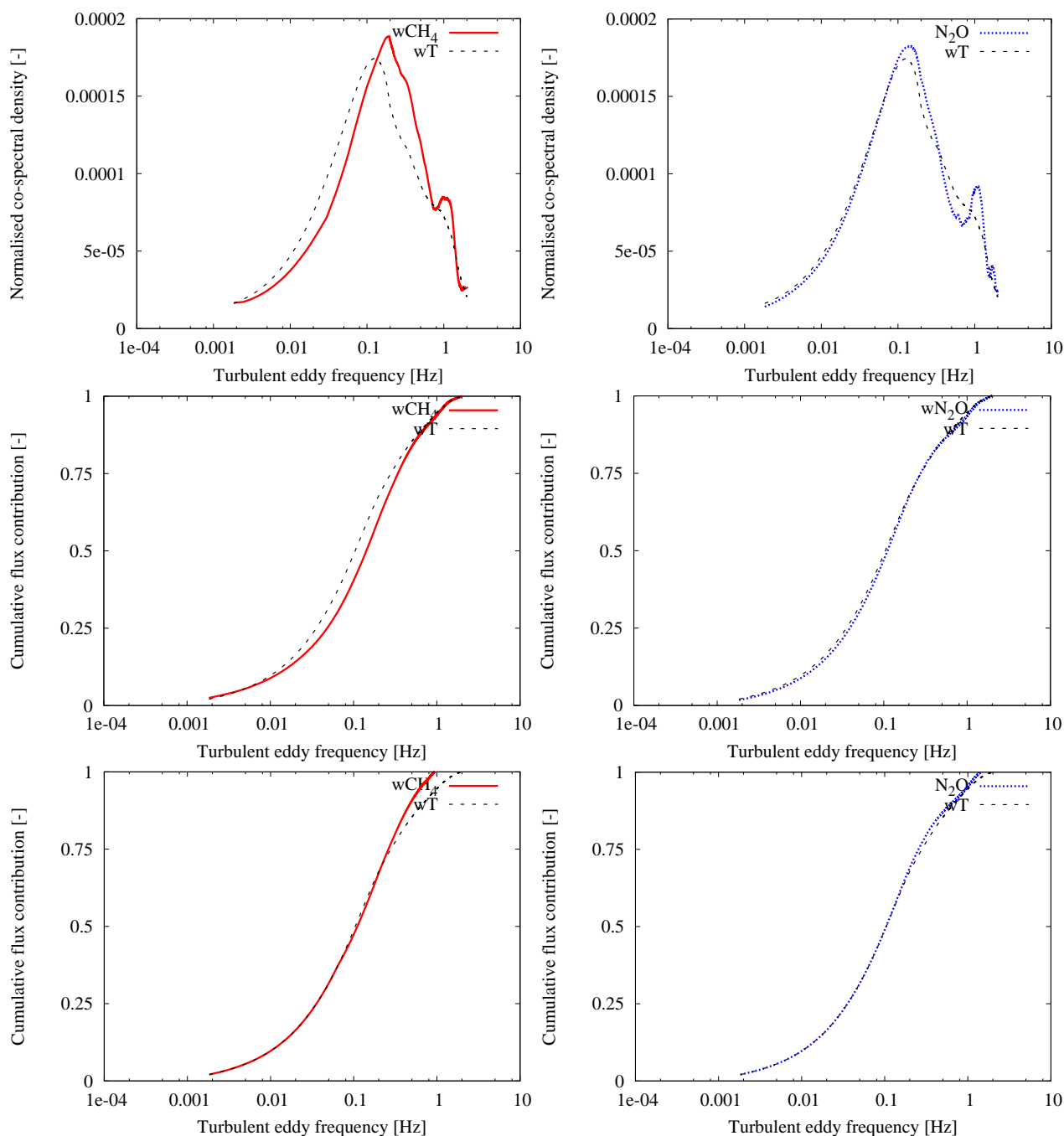


Fig. 3. Comparison of the absolute normalized co-spectra (top), unscaled (middle) and scaled ogives (bottom) with integration started from low frequencies of the heat and CH₄ flux (left) and the heat and N₂O flux (right). The given co-spectra and ogives represent averages over 4 half-hourly measurements on 8 October 2006 between 00:00–02:00.

improved by optimizing the least-squares fitting routines to minimize residuals between data and fit, and by optimizing the optical alignment of the system. Optical inference fringes, which can lead to instabilities with continuous wave laser systems, are not as important in pulsed laser systems. However, since the pulsed laser is operated near threshold

to maintain a narrow laser width, the short term precision is generally limited by detector noise. The influence of alignment and therefore the amount of laser power on the detector was investigated using laboratory tests. It was found that the precision was doubled when power at the detector was doubled by alignment optimization. The precision is

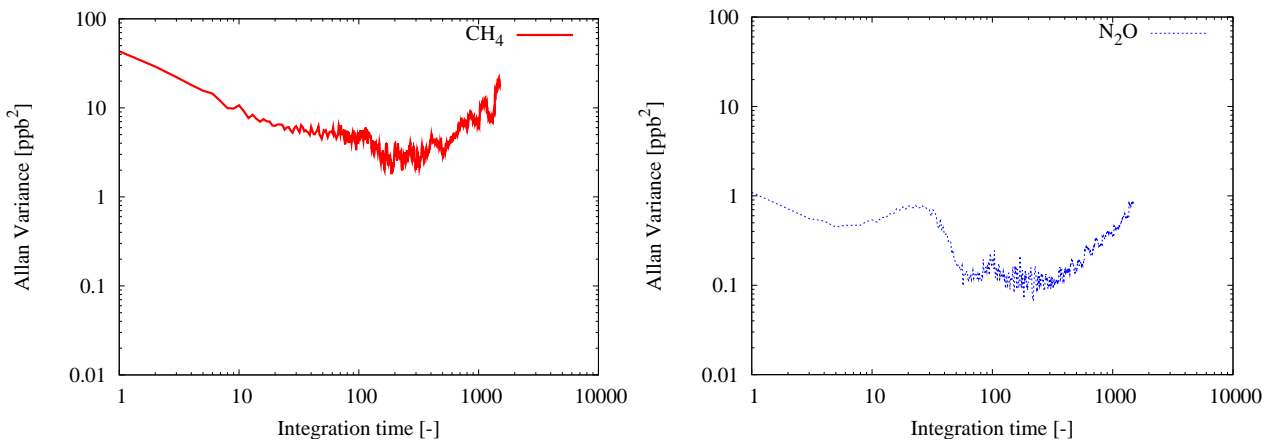


Fig. 4. Allan variance plots for CH₄ (left) and N₂O (right) during 14 min data period with 10 Hz sampling rate of ambient air from gasbags.

determined in the field using three ten liter gasbags filled with ambient air. The Allan variances are determined using 14 min of 10 Hz data. A precision of 2.9 ppb Hz^{-1/2} and 0.5 ppb Hz^{-1/2} for CH₄ and N₂O is derived using Fig. 4. These values are close to the required precision values of 4 ppb Hz^{-1/2} and 0.3 ppb Hz^{-1/2} which are given in Sect. 1. Our field values are also close to the precision values stated by Nelson et al. (2004). If a TE-cooled detector was used instead of a LN₂-cooled detector, the precision would probably decrease with a factor of three with the presently available detectors (Nelson et al., 2004).

The fourth criteria, the stationarity criteria, required intermediate term stability against span and minimal drift during a period of atmospheric stationarity on the order of 30 min. This validation consisted of two parts, namely the effect of the drift and the instrument adjustments on the stationarity. The minimum in the Allan variance defining the long-term stability which can be reached using this instrument is now about 200 s (Nelson et al., 2004). This minimum was determined in the laboratory. The long term stability of 10 s and longer can be worse in the field than in the laboratory where the temperature may not be controlled as well. In our case, the minimum was reached after 30 s (Fig. 4). However, CH₄ and N₂O fluxes are often calculated over an average time of 30 min. The choice of this interval is mainly based on the measurement height and the stability of the atmosphere since the size of the contributing eddies depends on those properties. Larger eddies contribute when the measurement height becomes higher and the atmospheric circumstances are more unstable. An over- or underestimation of flux can be caused by instrumental drift effects on time scales from 200 s to the longest average time of 30 min. This extra contribution only occurs when the fluctuations of the concentration are correlated with the fluctuations of the vertical wind velocity.

A running mean filter is a possible solution to filter drift contributions. A running mean filter with a time constant

equal to τ_A can be used. Nevertheless, this filter could cause an under- or overestimation of the flux due to filtering the contributions of large eddies since passive scalars, like CH₄ and N₂O, can acquire mesoscale fluctuations. These mesoscale fluctuations can occur while the convective process, which drives their advection, itself fluctuates on a horizontal scale on the order of the boundary layer, i.e. within the microscale range (Jonker et al., 1999).

An estimate of the under- or overestimation was made by means of ogive analyses based on Lee et al. (2004). In this case, the ogives were determined by integrating the absolute normalized co-spectrum starting from the high frequencies. This ogive is defined by

$$Og_{wc}^F(f_m) = \sum_{i=m}^{\frac{(n_s-1)\Delta t}{2\Delta t}} |Co_{wc}(f_i)|$$

$$f_i = \frac{i}{(n_s - 1)\Delta t}; m = 1, 2, \dots, \left[\frac{(n_s - 1)\Delta t}{2\Delta t} \right]. \quad (10)$$

The absolute normalized co-spectra were calculated over one hour starting at 7 October 2006 12:00 and 13:00 for CH₄ and N₂O using block averaging. The average normalized co-spectra were determined for each component over the two one-hourly co-spectra (Fig. 5). The amount of under- or overestimation was derived using the $Og_{wc}^F(8.3 \times 10^{-3})$ in which the frequency 8.3×10^{-3} Hz corresponds to the used running mean time constant of 120 s (Fig. 5).

It was derived that the underestimation due to the 120 s running mean filter was 11% and 8% for CH₄ and N₂O during this period. Besides, it was checked if the average time of 30 min was long enough to include all the contributed eddies to the flux. This validation was done by comparing the Og_{wc}^F values of the frequencies 3.0×10^{-4} and 6.1×10^{-4} Hz, which correspond to a time scale of 56 and 27 min, respectively. The difference was only 1%, therefore it was proved that an average time of 30 min was long enough in this case.

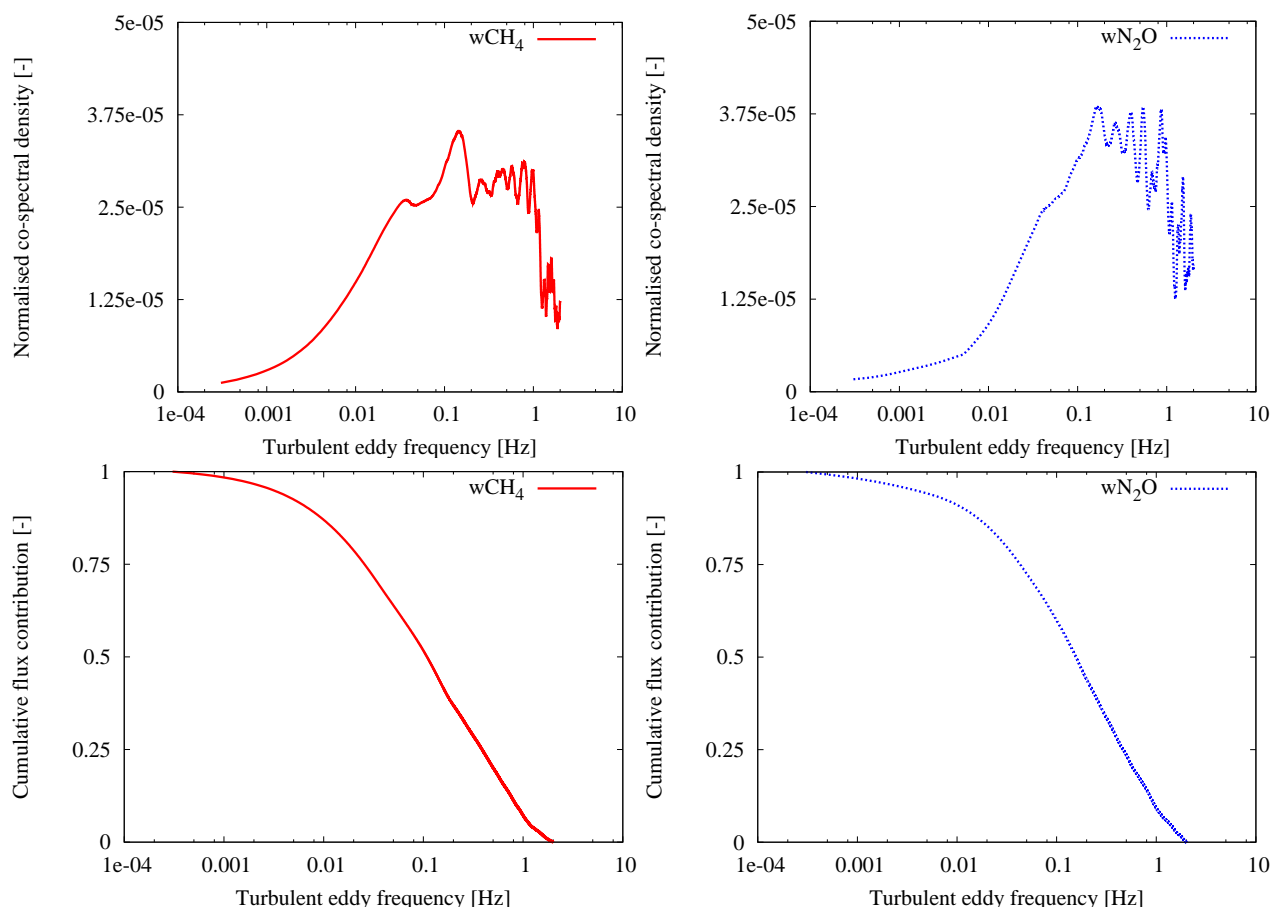


Fig. 5. The absolute normalized co-spectra and ogives with integration started from high frequencies of CH₄ flux (left) and N₂O flux (right) for determining the effect of the running mean filter and average time. The given ogives represent averages over 2 one-hourly measurements on 7 October 2006 between 12:00–14:00.

Although, more research should be done to derive the amount of underestimation due to the running mean and the minimal required average time for all circumstances.

Calibrations have to be performed to improve the accuracy of the mixing ratio values and therefore the accuracy of the flux values. Three different correction factors were calculated a low, a high and a low-high calibration factor. The low-high calibration was defined by Eq. (2) and both other factors were determined by

$$f_L = \frac{S_L}{M_L} \quad (11)$$

$$f_H = \frac{S_H}{M_H}. \quad (12)$$

The corrected concentration was found using one of these factors and the following equation

$$C_{\text{cor}} = f_x C_{\text{uncor}} \quad (13)$$

with f_x the low, high or low-high calibration factor, C_{uncor} the uncorrected concentration value in ppb and C_{cor} the cor-

rected concentration value in ppb. The low, high, and low-high calibration factors differ a lot (Fig. 6). This figure is based on an experiment with which the three calibration factors are determined by different cell pressures. It can be seen that a single point calibration with one-standard can provide flux values that differ by up to 18% from a two-standard estimate. By means of this, it can be stated that there will be a zero offset in our measurement system. Therefore, it will better to use a low-high calibration factor since the zero-offset should be the same for both. The lowest standard should be lower than the lowest expected atmospheric concentration and the highest standard should be higher than the highest expected concentration. Besides, the calibration factor will be more precise when more calibration standards are used. Only two standards are used in our case.

The calibration factor changed when instrument parameters were modified and when changes were made in fitting parameters or in alignment. The calibration factor seems to be slightly dependent on the cell pressure (Fig. 6). Therefore, it will be important to perform the calibrations at the pressure

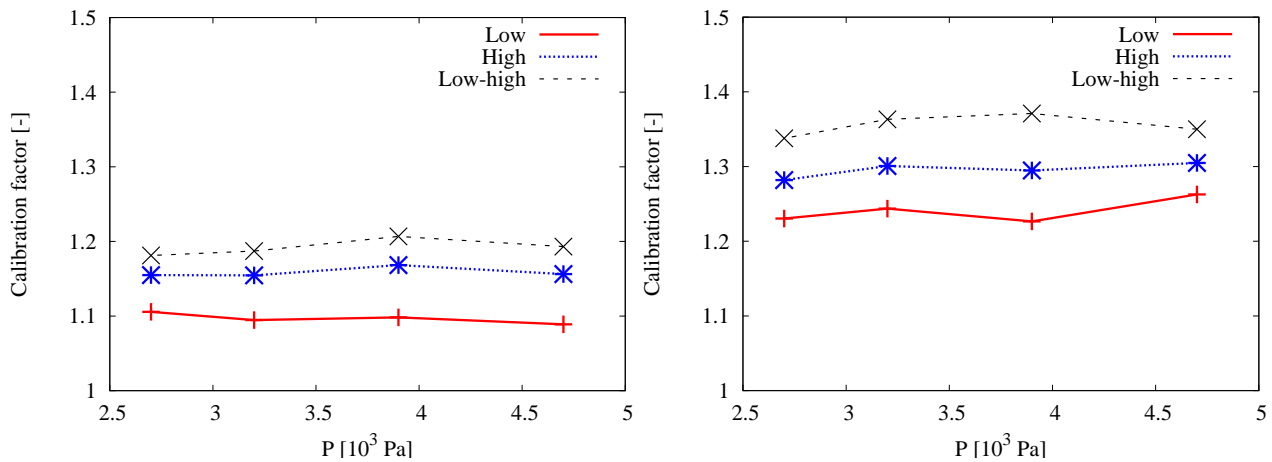


Fig. 6. Calibration factor as function of cell pressure for CH₄ (left) and N₂O (right).

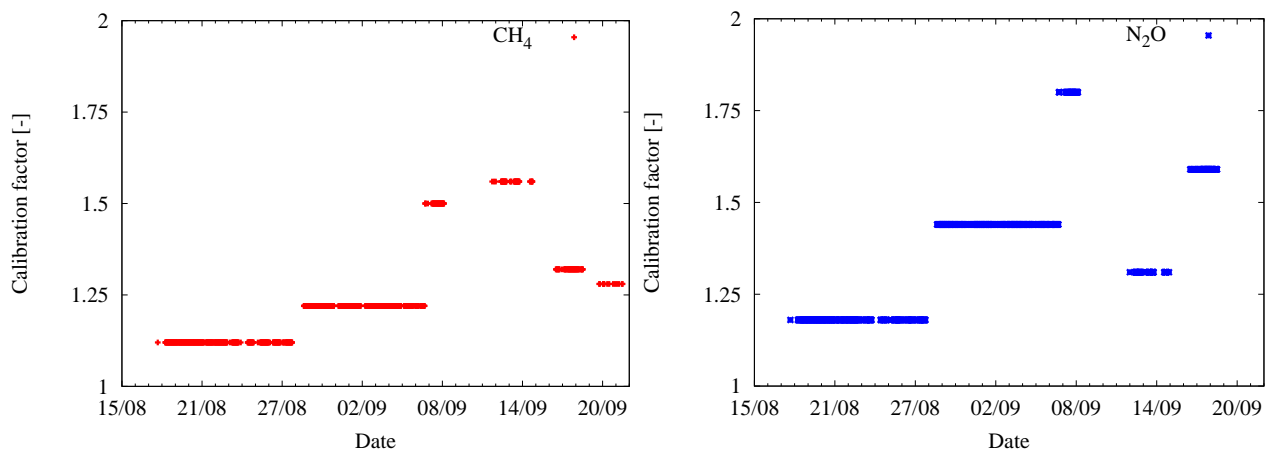


Fig. 7. Calibration factor of CH₄ (left) and N₂O (right) from 17 August to 22 September 2006. The cell pressure was nearly constant at 5.3×10^3 Pa (40 Torr) during this period.

of the measurements. The uncertainty in calibration factor will be a minor effect when a match of about 0.4×10^3 Pa is obtained. This match can easily be obtained. The calibration factor is more dependent on the alignment and the fitting parameters. The maximal difference in calibration factor was 0.44 and 0.63 for CH₄ and N₂O, respectively, based on data from 17 August until 22 September 2006 (Fig. 7). The cell pressure was nearly constant 5.3×10^3 Pa (40 Torr) during this period. These calibration factors were based on manual calibrations which were performed each field visit. Automatic calibrations will be better, however, they could not be performed until now.

4.2 CH₄ and N₂O exchange rates

4.2.1 Analysis using 30 min flux values

A dataset of CH₄ and N₂O EC measurements was obtained from 17 August to 6 November 2006 for which 99.8% was within the footprint of the investigated dairy farm site. About 7% of the CH₄ and 22% of the N₂O flux values were rejected by the instationarity tests (Foken and Wichura, 1996). The average standard deviations over six 5 min flux values were 84% and 185% for CH₄ and N₂O, respectively. So, the temporal variation was very large for both greenhouse gasses and especially for N₂O. The accepted calibrated and Webb-corrected 30 min NEE values are shown in Fig. 8.

In general the measurements for both CH₄ and N₂O show a net emission. About 98% and 91% of all flux values are positive for CH₄ and N₂O. In consequence, negative

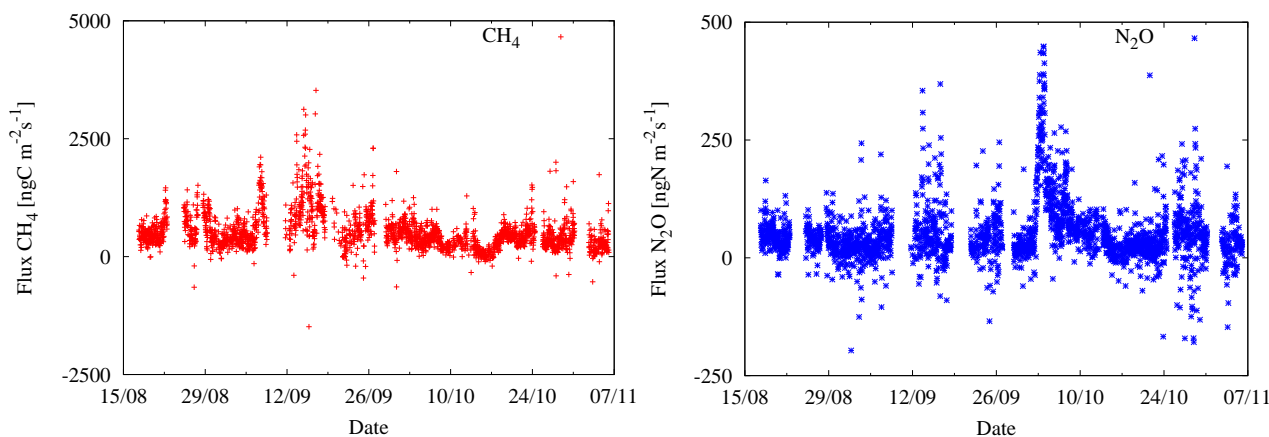


Fig. 8. 30 min flux values of CH₄ (left) and N₂O (right) from a dairy farm site in the Netherlands from 17 August to 6 November 2006.

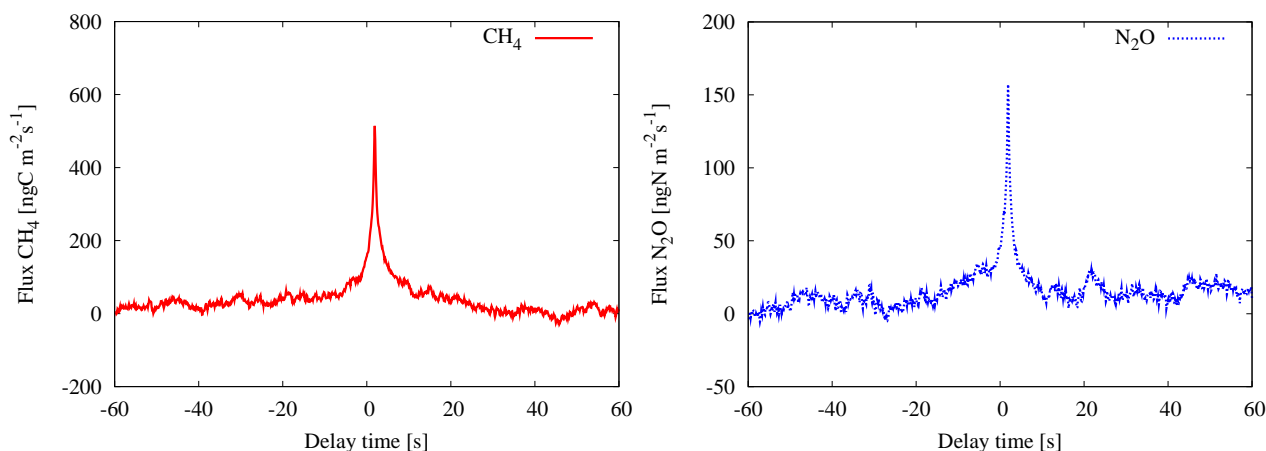


Fig. 9. Correlation versus delay time plots for CH₄ (left) and N₂O (right). The correlation plots represent averages over 4 half-hourly measurements on 7 October 2006 between 12:00–14:00.

fluxes also occurred, however, the reliability should be analyzed in more detail to investigate if these fluxes were not caused by an instrumental artifact. Most fluxes were between $-1000 \text{ ngC m}^{-2} \text{ s}^{-1}$ and $1000 \text{ ngC m}^{-2} \text{ s}^{-1}$ for CH₄ or between $-100 \text{ ngN m}^{-2} \text{ s}^{-1}$ and $100 \text{ ngN m}^{-2} \text{ s}^{-1}$ for N₂O. The high positive peaks were clearly related to cow manure application. The negative fluxes occurred in short events lasting at most a few hours. The negative CH₄ fluxes mainly occurred during low turbulence conditions with a friction velocity lower than 0.2 m s^{-1} . This was not the case for the negative N₂O fluxes. Therefore, most of the negative CH₄ fluxes will be filtered when u^* -filtering is applied.

The reliability of the negative fluxes was checked by a determination of the detection limit. The detection limit of the QCL spectrometer was derived using a method proposed by Wienhold et al. (1995). In this method, the standard deviation of the covariance function far outside the true lag time

is used as the estimation. An example of a covariance function is plotted in Fig. 9. The average detection limit of the QCL spectrometer was $41 \text{ ngC m}^{-2} \text{ s}^{-1}$ and $6 \text{ ngN m}^{-2} \text{ s}^{-1}$ based on all 30 min flux values with a clear defined peak in the correlation plot. Thus, the estimated detection limit was probably most of the time much smaller than the measured CH₄ and N₂O fluxes.

The conclusion is that large emissions of CH₄ and N₂O occurred at this dairy farm on peat grasslands. Moreover, negative emissions seemed to occur, however, more analyses should be performed to ascertain these uptakes. First, the raw data screening could be improved using an automatic screening based on the Vickers and Mahrt method (Vickers and Mahrt, 1997). Second, the negative fluxes should be analyzed using spectral analysis. For the net annual exchange, the uptake episodes were negligible.

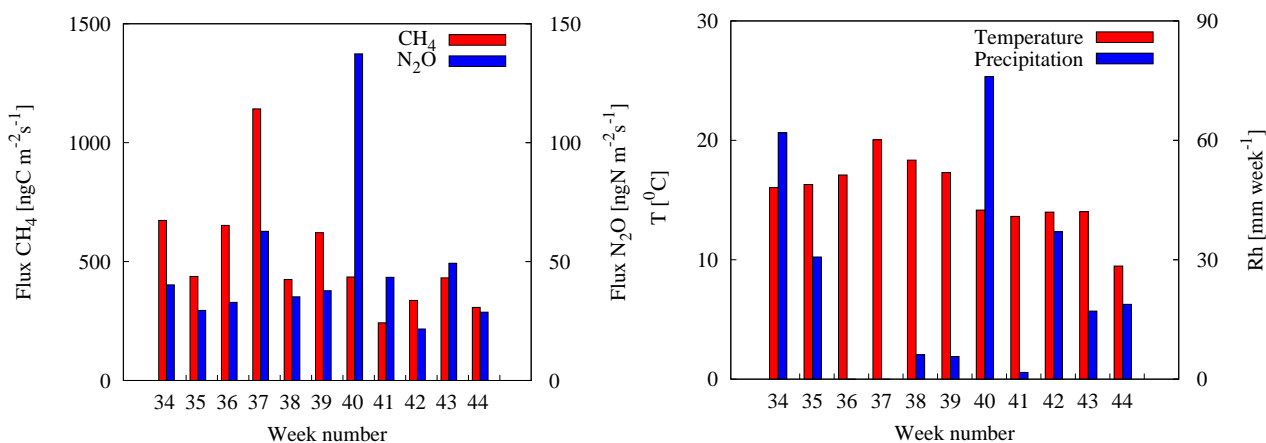


Fig. 10. Weekly average of CH_4 flux (left columns in red) and weekly average of N_2O flux (right columns in blue) in left figure, and weekly average of air temperature (left columns in red) and weekly precipitation rates (right columns in blue) in right figure measured at a dairy farm site in the Netherlands.

Table 2. Average and standard deviation of CH_4 and N_2O exchange at a dairy farm in the Netherlands over the period 17 August to 6 November 2006.

	CH_4 [$\text{ngC m}^{-2}\text{s}^{-1}$]	CH_4 [$\text{mg m}^{-2}\text{hr}^{-1}$]	N_2O [$\text{ngN m}^{-2}\text{s}^{-1}$]	N_2O [$\text{mg m}^{-2}\text{hr}^{-1}$]
NEE non-calibrated with Webb-correction	407 ± 281	1.95 ± 1.35	36 ± 47	0.20 ± 0.27
NEE calibrated with Webb-correction	512 ± 385	2.46 ± 1.85	52 ± 69	0.29 ± 0.39

4.2.2 Analysis using weekly flux values

Weekly average flux values were calculated when data coverage higher than 50% occurred in more than four days a week. An overview of weekly average CH_4 flux and N_2O flux are presented in Fig. 10. The weekly average air temperature and the weekly precipitation rates are also shown in Fig. 10. These have been made available by KNMI in the Netherlands. Cow manure was applied in week 37. The highest CH_4 weekly average flux also occurred in this week. The highest N_2O flux took place in week 40 after a large amount of precipitation.

4.2.3 Analysis using three months of flux values

The average calibrated corrected NEE and the standard deviation in the average were $512 \pm 385 \text{ ngC m}^{-2} \text{ s}^{-1}$ and $52 \pm 69 \text{ ngN m}^{-2} \text{ s}^{-1}$ from which 40% of N_2O emission was due to the fertilizing event. Thus, the standard deviations were of the same order of the average flux values, this was mainly caused by the fertilizing event. The calibrated NEE was about 26% and 44% higher than the non-calibrated NEE for CH_4 and N_2O , respectively.

The Webb-corrected NEE was 6% higher for CH_4 and 34% higher for N_2O than the non-Webb-corrected NEE.

The Webb-correction is probably somewhat lower since the correction is based on a near located open path system. However, the calibrated NEE values with Webb-correction seemed to be a good first estimation of the CH_4 and N_2O exchange at this dairy farm on peat land since the overestimation of the Webb-correction is probably compensated by the underestimation due to the damping effect and the use of a running mean filter. A summary of non-calibrated Webb-corrected NEE and calibrated Webb-corrected NEE is given in Table 2.

5 Conclusions

A QCL was used for EC measurements of CH_4 and N_2O . Evaluation of its performance was performed using three months of continuous measurements at a dairy farm site on peat land in the Netherlands. The required criteria for eddy covariance flux measurements including continuity, sampling frequency, precision and stationarity were examined. The system operated continuously from 17 August to 6 November 2006 with about one visit a week. The validation of the sampling frequency of the system consisted of three parts, namely the electronic sampling frequency, the flow response and the damping. An electronic sampling

frequency of 10 Hz was obtained using a 1 GHz PC system. The flow response time was about 2 Hz and almost no damping to the flux contribution by the high frequency eddies occurred. Thus, the overall sampling frequency of the system was about 2 Hz. A precision of $2.9 \text{ ppb Hz}^{-1/2}$ and $0.5 \text{ ppb Hz}^{-1/2}$ was obtained for CH_4 and N_2O , respectively. These values are close to the required precision values of $4 \text{ ppb Hz}^{-1/2}$ and $0.3 \text{ ppb Hz}^{-1/2}$. The precision was strongly dependent on the power on the detector and thus the alignment. The stationarity was checked using Allan variance analyses and frequently calibration sessions. Drift in the system was removed using a 120 s running mean filter. A two-point calibration was required at least once a week.

The continuous operation of the system was also proven by three months of field measurements (data coverage of 87%). A first estimate of CH_4 and N_2O exchange was made. The average calibrated corrected exchange was $512 \text{ ngC m}^{-2} \text{ s}^{-1}$ and $52 \text{ ngN m}^{-2} \text{ s}^{-1}$ for CH_4 and N_2O , respectively, from which 40% of N_2O emission was due to the fertilizing event. The N_2O peak, which was strongly correlated to precipitation, occurred about three weeks after the fertilizing. Finally, although the dairy farm site was a net source of CH_4 and N_2O , uptake also seemed to occur in short events lasting at most a few hours. However, more research should be done to investigate the reliability of these negative fluxes.

In conclusion, a QCL spectrometer was suitable for performing continuous EC measurements of CH_4 and N_2O . Nevertheless, a two-point calibration was necessary for obtaining accurate estimates. Besides, the possible underestimation due to the damping effect, the use of a running mean filter and the limited effective sampling frequency should be analyzed in more detail.

Acknowledgements. This research was part of the Dutch National Research Program BSIK ME1. Thanks are due to our colleagues P. van den Bulk, P. Fonteijn and T. Schrijver for their assistance during setting-up these experiments. We are also very grateful to E. Veenendaal of University of Wageningen for making available the latent heat flux data. Our thanks are also due to E. de Beus of Technical University of Delft for his assistance in data analyses. Finally, we owe a special debt of gratitude to the farmer T. van Eyk for using his farm site.

Edited by: A. Neftel

References

- Allan, D. W.: Statistics of atomic frequency standards, Proceedings of the IEEE, 54, 221–230, 1966.
- Ammann, C.: On the applicability of relaxed eddy accumulation and common methods for measuring trace gas surface fluxes, Diss. ETH No. 12795, Zurich, 1998.
- Ammann, C., Brunner, A., Spirig, C., and Neftel, A.: Technical note: Water vapour concentration and flux measurements with PTR-MS, Atmos. Chem. Phys., 6, 4643–4651, 2006, <http://www.atmos-chem-phys.net/6/4643/2006/>.
- Eugster, W., Zeyer, K., Zeeman, M., Michna, P., Zingg, A., Buchmann, N., and Emmenegger, L.: Nitrous oxide net exchange in a beech dominated mixed forest in Switzerland measured with a quantum cascade laser spectrometer, Biogeosciences Discuss., 4, 1167–1200, 2007, <http://www.biogeosciences-discuss.net/4/1167/2007/>.
- Faist, J., Capasso, F., Sivco, D. L., Sirtori, C., Hutchinson, A. L., and Cho, A. Y.: Quantum cascade laser, Science, 264, 553–556, 1994.
- Foken, T. and Wichura, B.: Tools for quality assessment of surface-based flux measurements, Agr. Forest Meteorol., 78, 83–105, 1996.
- Hargreaves, K. J., Fowler, D., Pitcairn, C. E. R., and Aurela, M.: Annual methane emission from Finnish mires estimated from eddy covariance campaign measurements, Theor. Appl. Climatol., 70, 203–213, 2001.
- Hoogendoorn, C. J. and van der Meer, T. H.: Fysische transportverschijnselen II, Delftse Uitgevers Maatschappij, Delft, The Netherlands, 1991.
- IPCC: Climate change 2001, The Scientific Basis, Cambridge University Press, Cambridge, UK, 2001.
- IPCC: Climate change 1995, Scientific and technical analyses of impacts, adaptations and mitigation. Contribution of working group II to the Second Assessment Report of the Intergovernmental Panel on Climatic Change, Cambridge University Press, London, 2006.
- Jiménez, R., Herndon, S., Shorter, J. H., Nelson, D. D., McManus, J. B., and Zahniser, M. S.: Atmospheric trace gas measurements using a dual quantum-cascade laser mid-infrared absorption spectrometer, Proceedings of SPIE, 5738, 318–331, 2005.
- Jonker, H. J. J., Duynkerke, P. G., and Cuijpers, J. W. M.: Mesoscales fluctuations in scalars generated by boundary layer convection, J. Atmos. Sci., 56, 801–808, 1999.
- Kaimal, J. C. and Finnigan, J. J.: Atmospheric boundary layer flows, Oxford University Press, Oxford, 1994.
- Kormann, R. and Meixner, F. X.: An analytical footprint model for non-neutral stratification, Bound.-Lay. Meteorol., 99, 207–224, 2001.
- Laville, P., Jambert, C., Cellier, P., and Delmas, R.: Nitrous oxide fluxes from a fertilized maize crop using micrometeorological and chamber methods, Agr. Forest Meteorol., 96, 19–38, 1999.
- Lee, X. L., Massman, W., and Law, B.: Handbook of micrometeorology, Kluwer Academic Publishers, Dordrecht, The Netherlands, 2004.
- Lenschow, D. H. and Mann, J.: How long is long enough when measuring fluxes and other turbulent statistics?, J. Atmos. Ocean. Tech., 11, 661–673, 1994.
- McMillen, R. T.: An eddy correlation technique with extended applicability to non-simple terrain, Bound.-Lay. Meteorol., 43, 231–245, 1988.
- Monteith, J. L. and Unsworth, M. H.: Principles of environmental physics, Edward Arnold, London, 1990.
- Neftel, A., Flechard, C., Ammann, C., Conen, F., Emmenegger, L., and Zeyer, K.: Experimental assessment of N_2O background fluxes in grassland systems, Tellus B, 59, 470–482, 2007.
- Nelson, D. D., Shorter, J. H., McManus, J. B., and Zahniser, M. S.: Sub-part-per-billion detection of nitric oxide in air using a thermoelectrically cooled mid-infrared quantum cascade laser spectrometer, Appl. Phys. B, 75, 343–350, 2002.

- Nelson, D. D., McManus, B., Urbanski, S., Herndon, S., and Zahniser, M. S.: High precision measurements of atmospheric nitrous oxide and methane using thermoelectrically cooled mid-infrared quantum cascade lasers and detectors, *Spectrochimica Acta Part A*, 60, 3325–3335, 2004.
- Nieuwstadt, F. T. M.: *Turbulentie*, Epsilon Uitgaven Utrecht, Utrecht, The Netherlands, 1998.
- Rothman, L. S. and Barbe, A.: The HITRAN molecular spectroscopic database: edition of 2000 including updates through 2001, *Journal of Quantitative Spectroscopy and Radiative Transfer*, 82, 5–44, 2003.
- Smith, K. A., Clayton, H., Arah, J. R. M., Christensen, S., Ambus, P., Fowler, D., Hargreaves, K. J., Skiba, U., Harris, G. W., Wienhold, F. G., Klemetsson, L., and Galle, B.: Micrometeorological and chamber methods for measurement of nitrous oxide fluxes between soils and the atmosphere: Overview and conclusions, *J. Geophys. Res.*, 99, 16 541–16 548, 1994.
- Veenendaal, E. M., Kolle, O., Leffelaar, P., Schrier-Uijl, A. P., van Huissteden, J., van Walsem, J., Möller, F., and Berendse, F.: Land use dependent CO₂ exchange and carbon balance in two grassland sites on eutropic drained peat soils, *Biogeosciences Discuss.*, 4, 1633–1671, 2007, <http://www.biogeosciences-discuss.net/4/1633/2007/>.
- Vickers, D. and Mahrt, L.: Quality control and flux sampling problems for tower and aircraft data, *J. Atmos. Ocean. Tech.*, 14, 512–526, 1997.
- Webb, E. K., Pearman, G. I., and Leuning, R.: Correction of flux measurements for density effects due to heat and water vapour transfer, *Q. J. Roy. Meteor. Soc.*, 106, 85–100, 1980.
- Werle, P. and Kormann, R.: Fast chemical sensor for eddy-correlation measurements of methane emissions from rice paddy fields, *Appl. Opt.*, 40, 846–858, 2001.
- Werle, P. and Slemr, F.: Signal-to-noise ratio analysis in laser absorption spectrometers using optical multipass cells, *Appl. Opt.*, 30, 430–434, 1991.
- Wienhold, F. G., Frahm, H., and Harris, G. W.: Measurements of N₂O fluxes from fertilized grassland using a fast response tunable diode laser spectrometer, *J. Geophys. Res.*, 99, 16 557–16 567, 1994.
- Wienhold, F. G., Welling, M., and Harris, G. W.: Micrometeorological measurement and source region analysis of nitrous oxide fluxes from an agricultural soil, *Atmos. Environ.*, 29, 2219–2227, 1995.